Int. J. Heat Mass Transfer. Vol. 35, No. 4, pp. 823–832, 1992
Printed in Great Britain

0017-9310/92 $5.00+0.00
Pergamon Press plc

Mixed convection heat transfer from the bottom tip of a cylinder spinning about a vertical axis in a saturated porous medium

R. V. KAMATH,† M. R. RAVI‡ and A. G. MARATHE†

†Department of Aerospace Engineering, Indian Institute of Technology, Bombay 400076, India

‡Department of Mechanical Engineering, Indian Institute of Science, Bangalore 560012, India

(*Received* 21 *May* 1990 *and in final form* 19 *December* 1990)

Abstract—The present work is a numerical study of heat transfer characteristics from the bottom tip of a cylinder spinning about a vertical axis in an infinitely saturated porous medium. The problem is axisymmetric. The non-dimensionalized governing equations are solved using the SIMPLER algorithm on a staggered grid. The influence of rotational Reynolds numbers and Darcy numbers on the heat transfer for a Grashof number of 10^4 and Prandtl number of 7.0 is studied. It is found that for very high Darcy numbers, over a wide range of rotational Reynolds numbers, the heat transfer takes place mainly due to conduction. The convective heat transfer takes place for lower Darcy numbers and for higher rotational Reynolds numbers. Moreover, there is a rapid increase in the overall Nusselt number below a certain Darcy number with increase in the rotational Reynolds numbers. The effect of the Darcy number and the rotational Reynolds number on the heat transfer and fluid flow in the porous medium is depicted in the form of streamline and isotherm plots. The variation of the overall Nusselt number with respect to the Darcy number for various rotational Reynolds numbers is plotted. The variation of the local Nusselt number with respect to the radial coordinate at the heated tip of the vertical cylinder is plotted for various Darcy and rotational Reynolds numbers.

INTRODUCTION

CONVECTIVE heat transfer in saturated porous media has been gaining importance in recent years, both in academic and in practical situations. Considerable attention has been paid to achieve greater understanding of the transport phenomena in saturated porous media subjected to free, forced, and mixed convection. The prediction of natural convective heat transfer characteristics from heated bodies embedded in a porous medium is of great practical significance, especially in geothermy, nuclear waste disposal, heat pipe technology, mining, underground gas pipes and in the petroleum industry.

In the recent past, considerable numerical work has been reported on natural, as well as forced, convection inside a saturated porous medium. Most of the reported work is based on the Darcy law of fluid flow inside the porous medium. Free convective heat transfer about a vertical cylinder has been solved using the boundary layer approximation [1]. The surface temperature of the cylinder is varied as a power function of the distance from the leading edge. Thermal convection in a saturated porous medium bounded by two horizontal cylinders is numerically simulated for low Rayleigh numbers [2, 3]. The fluid motion is assumed to be described by the Darcy–Oberseck–Boussinesq equation. An experimental work has also been reported for natural convective heat transfer in concentric and eccentric horizontal annuli [4] in a porous medium. Mixed convection flow inside a saturated porous medium has been solved by using the general transformation [5]. The effect of boundary and inertia on flow and heat transfer in a porous medium has been studied [6].

When permeability of the porous medium is high, the Darcy law of fluid flow does not hold good. Many workers have used the Darcy equation with Brinkmann's modification [7]. In the present work, natural convective heat transfer from the tip of a drilling cutter spinning inside a saturated porous medium is numerically simulated. This is a frequently encountered problem in foundation, bore well and oil well drilling. Brinkmann's modified Darcy equation along with the continuity and energy equations are solved for velocity, pressure and temperature distributions. The SIMPLER algorithm [9] is employed to handle the velocity–pressure coupling.

FORMULATION

The drill shaft is assumed to be a semi-infinite cylinder, spinning inside an infinitely saturated porous medium. The tip of the cylinder is assumed to be at a constant temperature. In the drilling process there is always a certain gap between the wall of the cylinder and the earth, through which water is forced in order to minimize friction. As a result, there is a formation of a thin layer of fluid. This layer offers resistance to heat transfer from the cylinder to the external medium. To take this fact into account the circumference of the cylinder along the length is assumed to be insulated. The saturated porous medium is assumed to be homogeneous and to have constant properties. The fluid and the porous material are

NOMENCLATURE

a	radius of the rod
g	acceleration due to gravity
k	effective thermal conductivity of the saturated porous medium
K	permeability of the porous medium
P	pressure
r	radial coordinate
S	general non-dimensional source term
T	temperature
T_∞	temperature at infinity
T_{tip}	temperature at the cylinder tip
ΔT	temperature difference, $(T_{tip} - T_\infty)$
u	radial velocity
v	azimuthal velocity
w	axial velocity
z	axial coordinate.

Greek symbols

α	effective thermal diffusivity
β	coefficient of cubic thermal expansion
Γ	general non-dimensional diffusion coefficient
ν	effective momentum diffusivity
ρ	density of the fluid
Φ	general non-dimensional variable
Ω	angular velocity of the cylinder.

Non-dimensional parameters

Da	Darcy number, a^2/K
Gr	Grashof number, $g\beta\Delta Ta^3/\nu^2$
Nu	Nusselt number, ha/k
P	pressure, $pa^2/\rho\nu^2$
Pr	Prandtl number, ν/α
R	radial coordinate, r/a
U	radial velocity, ua/ν
V	azimuthal velocity, va/ν
Vo	rotational Reynolds number, $a^2\Omega/\nu$
W	axial velocity, wa/ν
Z	axial coordinate, z/a
Θ	non-dimensional temperature, $(T - T_\infty)/\Delta T$.

assumed to be in local thermodynamic equilibrium. Heat is generated due to the friction only at the tip of the cylinder. It is assumed that there is no temperature gradient inside the cylinder.

The free convective heat transfer due to the hot cylinder tip, the forced convective heat transfer due to the rotation of the cylinder, and the resulting mixed convective heat transfer due to the interaction of the above phenomena are studied numerically. Since the present problem is axisymmetric in nature, the equations are solved on an axisymmetric (R–Z) plane. The computational domain is rectangular as shown in Fig. 1. The limiting values of r_{max}, z_{min} and z_{max} were chosen

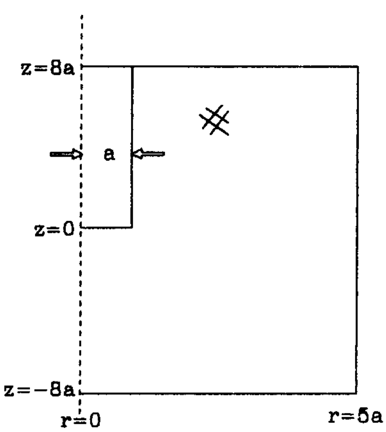

FIG. 1. Computational domain.

such that the variables in the interior of the domain remained independent of their values [8, 10]. It was found that $r_{max} = 5a$ in the radial direction and $z_{min} = -8a$ and $z_{max} = 8a$ in the axial direction satisfied the above requirements for the range of parameters investigated.

Infinity for the present problem is assumed to be the point where the velocity component along the boundary tends to zero. Hence at the r infinity boundary the axial component tends to zero, while at the z infinity boundaries the radial velocity tends to zero. Since only relative values of pressure are of interest in incompressible flow problems, and since the pressure has to be constant at the far field boundaries, pressure is assumed to be zero on these boundaries [8, 10]. The boundary conditions for the energy equation are based on the flow direction at the boundary. If the flow is into the domain, $T = T_\infty$ at the boundary, while $dT/dn = 0$ when the flow is outward, n being the coordinate normal at the boundary.

The governing equations are as follows:

continuity equation

$$\frac{1}{r}\frac{\partial(ur)}{\partial r} + \frac{\partial(w)}{\partial z} = 0; \tag{1}$$

radial momentum equation

$$\frac{1}{r}\frac{\partial(ruu)}{\partial r} + \frac{\partial(uw)}{\partial z} - \frac{v^2}{r} = -\frac{1}{\rho}\frac{\partial p}{\partial r} - \frac{\nu u}{K} + \nu\left[\frac{1}{r}\frac{\partial}{\partial r}\left(r\frac{\partial u}{\partial r}\right) - \frac{u}{r^2} + \frac{\partial^2 u}{\partial z^2}\right]; \tag{2}$$

azimuthal momentum equation

$$\frac{1}{r}\frac{\partial(ruv)}{\partial r}+\frac{\partial(vw)}{\partial z}-\frac{uv}{r}=-\frac{vv}{K}+v\left[\frac{1}{r}\frac{\partial}{\partial r}\left(r\frac{\partial v}{\partial r}\right)-\frac{v}{r^2}+\frac{\partial^2 v}{\partial z^2}\right]; \quad (3)$$

axial momentum equation

$$\frac{1}{r}\frac{\partial(ruw)}{\partial r}+\frac{\partial(ww)}{\partial z}=-\frac{1}{\rho}\frac{\partial p}{\partial z}+g\beta(T-T_\infty)-\frac{vw}{K}+v\left[\frac{1}{r}\frac{\partial}{\partial r}\left(r\frac{\partial w}{\partial r}\right)+\frac{\partial^2 w}{\partial z^2}\right]; \quad (4)$$

energy equation

$$\frac{1}{r}\frac{\partial(ruT)}{\partial r}+\frac{\partial(wT)}{\partial z}=\alpha\left[\frac{1}{r}\frac{\partial}{\partial r}\left(r\frac{\partial T}{\partial r}\right)+\frac{\partial^2 T}{\partial z^2}\right]. \quad (5)$$

The boundary conditions for the momentum equations and energy equation are as follows:

$$r=0;\quad u=0,\quad v=0,\quad \frac{\partial w}{\partial r}=0$$

$$r=r_{\max};\quad \frac{\partial(ur)}{\partial r}=0,\quad v=0,\quad w=0$$

$$z=z_{\min};\quad u=0,\quad v=0,\quad \frac{\partial w}{\partial z}=0$$

$$z=z_{\max};\quad u=0,\quad v=0,\quad \frac{\partial w}{\partial z}=0$$

$$z=0;\quad 0<r\leqslant a;\quad u=0,\quad v=r\Omega,\quad w=0$$

$$r=0;\quad \frac{\mathrm{d}T}{\mathrm{d}r}=0,\quad r=r_{\max};\quad T=T_\infty,\quad u<0$$

$$z=z_{\min};\quad T=T_\infty,\quad w>0,\quad \frac{\partial T}{\partial z}=0,\quad w<0$$

$$z=z_{\max};\quad T=T_\infty,\quad w<0,\quad \frac{\partial T}{\partial z}=0,\quad w>0$$

$$z=0;\quad 0<r<a;\quad T=T_{\text{tip}}.$$

NUMERICAL PROCEDURE

The governing equations are non-dimensionalized using the radius of the cylinder a as the reference length and $(T_{\text{tip}}-T_\infty)$ as the reference temperature difference. The Boussinesq approximation is used on the axial momentum equation. The original equations (1)–(5) result in the following general conservation equation:

$$\frac{1}{R}\frac{\partial}{\partial R}\left[R\left(U\Phi-\Gamma_\Phi\frac{\partial\Phi}{\partial R}\right)\right]+\frac{\partial}{\partial z}\left[\left(W\Phi-\Gamma_\Phi\frac{\partial\Phi}{\partial Z}\right)\right]=S_\Phi \quad (6)$$

where Φ is the general variable, Γ_Φ the diffusion coefficient and S_Φ the source term corresponding to Φ in the different equations (1)–(5). These are listed in Table 1.

Table 1. Terms in the general equation

Equation	Φ	Γ_Φ	S_Φ
(1)	1	0.0	0.0
(2)	U	1.0	$-\frac{\partial P}{\partial R}+\frac{V^2}{R}-\frac{U}{R^2}-Pr\,Da\,U$
(3)	V	1.0	$-\frac{UV}{R}-\frac{V}{R^2}-Pr\,Da\,V$
(4)	W	1.0	$-\frac{\partial P}{\partial Z}+Gr\,\Theta-Pr\,Da\,W$
(5)	Θ	$1/Pr$	0.0

Algebraic equations are obtained by integrating the above general equation (6) over the control volumes on the staggered grid system for the respective variables. The discretization procedure proposed by Patankar and Spalding [11] and Patankar [9] has been employed. A power law variation of the variables has been assumed between the discrete points. The pressure and velocity correction and updating for successive iterations used in the present work follow the SIMPLER algorithm [9]. The grid size beyond which the solutions are grid independent was found to be 20×45. The grid sizes used were non-uniform and the smallest grid was $0.001a$ along the axial direction and $0.01a$ along the radial direction. The grid independence of the solutions was tested by running a typical case on a 40×73 non-uniform mesh. The resulting Nusselt numbers did not vary by more than 0.1%. The residue obtained from the continuity equation at all points was used as the convergence criterion. The value of the convergence criterion was 10^{-5}.

RESULTS AND DISCUSSION

The present problem is an attempt to numerically simulate the drilling process encountered in the petroleum industries and in civil engineering. The values of all the input parameters are realistic [12] and the range of these parameters used is shown in Table 2. The non-dimensional numbers are obtained from these sets of values for computation.

The results are presented in the form of streamline and isotherm plots. The present problem is axisymmetric, with the presence of a circumferential velocity. This means that the streamlines are, strictly speaking, three-dimensional. But the envelope of these streamlines forms axisymmetric stream tubes. The term 'streamlines' in this paper denotes the sectional lines of these stream tubes and not the actual streamlines. The mean Nusselt numbers are plotted against rotational Reynolds numbers for various Darcy numbers. The streamlines and isotherms are plotted for extreme Darcy and rotational Reynolds numbers.

Table 2. Range of parameters

S. No.	Parameters	Range	Units
(1)	Radius of the drilling rod (a)	10–20	cm
(2)	Permeability of the porous medium (K)	0.02–0.0001	cm^2
(3)	Angular velocity of the drill bit (Ω)	50–100	rev min^{-1}
(4)	Effective thermal diffusivity (α)	10^{-5} 10^{-6}	$m^2\ s^{-1}$

The stream function is defined as follows:

$$U = \frac{1}{R}\frac{\partial \Psi}{\partial Z}, \quad W = -\frac{1}{R}\frac{\partial \Psi}{\partial R}.$$

Figures 2 and 3 show the streamline–isotherm plots and local Nusselt number plot for a Darcy number of 10^6 and a rotational Reynolds number $Vo = 0$, respectively. Figures 4 and 5 show the streamline–isotherm plots and local Nusselt number plot for a Darcy number of 10^4 and a rotational Reynolds number $Vo = 0$, respectively. The above set of figures shows the significant effect of Darcy numbers on the streamlines and isotherms. There is an increase in the maximum stream function value. The heat transfer takes place mainly due to conduction for high Darcy numbers and convection for low Darcy numbers for a given Vo. This is because, since the fluid velocity is very low for high Darcy numbers, heat gets conducted through the saturated porous matrix in all directions. In other words, the heat transfer due to natural convection is negligible. Hence, the isotherms are nearly concentric circles in the two-dimensional view. As the Darcy number decreases, the fluid tends to move freely due to an increase in permeability resulting in an increase in heat transfer.

Figures 6 and 7 are streamline–isotherm plots and the local Nusselt number plot for a Darcy number of 10^6 and a rotational Reynolds number $Vo = 5000$, while Figs. 8 and 9 show the streamline–isotherm plots and local Nusselt number plot for a Darcy number of 10^4 and a rotational Reynolds number $Vo = 5000$, respectively. A comparison of Figs. 2 and 8 for a Darcy number of 10^4 shows that as the rotational Reynolds number increases the streamlines tend to drift towards the axis of the cylinder. Moreover, there is a formation of a small recirculation region below the tip of the cylinder. This can be explained as follows. As Vo increases so the tangential velocity of the fluid below the tip of the cylinder increases. This results in movement of the fluid in a radial direction pointing away from the axis of the cylinder. In order to make up for the depletion of the fluid at this region the fluid from below gets sucked towards this region. Hence, the streamlines get clustered near the tip of the cylinder, thus giving rise to a small region of recirculation. This phenomenon is more predominant for low Darcy numbers than for high Darcy numbers (see Fig. 6). There is a significant drop in the local Nusselt number along the radial direction, as shown in Fig. 9. This is due to the fact that the recirculation zone increases the resistance to heat transfer and hence there is a drop in the local Nusselt number at the tip.

A correlation of average Nusselt number, with respect to the Darcy number of the porous medium, and the rotational Reynolds number of the cylinder is obtained by using a least square fit on 156 data points for a Grashof number of 10^4 and a Prandtl number of 7.0. It was found to be of the form

$$Nu = a + (b + c\,Vo + d\,Vo^2)\,e^{-f\,Da}$$

where $a = 3.75358$, $b = 2.01$, $c = 0.2516 \times 10^{-4}$, $d = 0.00155$, and $f = 1.1 \times 10^{-4}$.

The correlation shows that the average Nusselt number is a parabolic function of the rotational Reynolds number Vo and a decaying exponential function of the Darcy number Da. As a result, for a very large number, the correlation loses the dependence of Vo and Da. Hence we get a constant value of the Nusselt number which is nothing but the conduction limit. On the other hand, for a very low Darcy number, the average Nusselt number becomes a function of Vo only. This becomes the case of a cylinder spinning in a pure fluid medium. Thus the proposed correlation can handle extreme cases. The conduction limit was validated against the ANSYS package. It was found that the Nusselt numbers predicted by the proposed correlation, and computed by using ANSYS, differ by 1.5%. However, for the pure convection limit, the authors know of no existing correlation of Nusselt number for validation. The fitted value of the Nusselt number using this correlation is found to be within 10% error of the computed value. Figure 10 shows the mean Nusselt number variation with respect to rotational Reynolds number for various Darcy numbers.

CONCLUSION

The heat transfer characteristics from the tip of a cylinder spinning about its vertical axis inside a saturated porous medium is studied numerically. The results show that the Nusselt number is a decaying exponential function of the Darcy number and a parabolic function of the rotational Reynolds number. Moreover, there is a significant increase in the mean Nusselt number below a certain Darcy number for a given Vo. The heat transfer takes place mainly due to conduction for low rotational speeds and convection

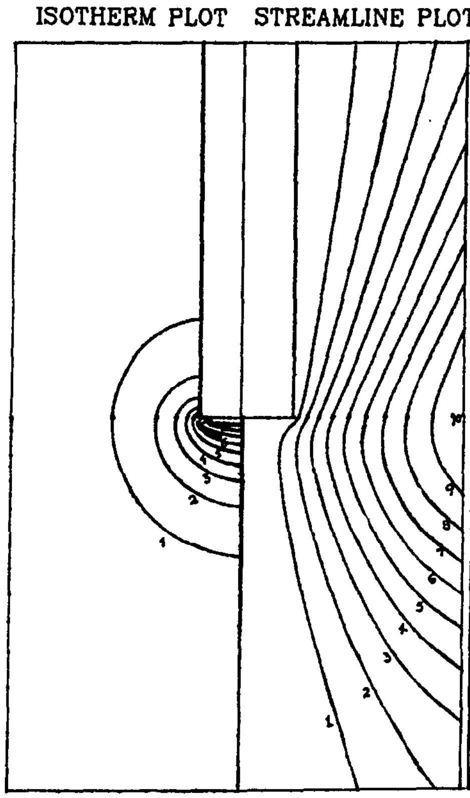

Contour Levels	ψ Values	θ Values
1.	1.37e−3	0.1
2.	2.74e−3	0.2
3.	4.11e−3	0.3
4.	5.48e−3	0.4
5.	6.85e−3	0.5
6.	8.85e−3	0.6
7.	9.59e−3	0.7
8.	1.09e−2	0.8
9.	1.23e−2	0.9
10.	1.37e−2	1.0

FIG. 2. Streamline and isotherm plot for $Gr = 10^4$, $Da = 10^6$ and $Vo = 0$.

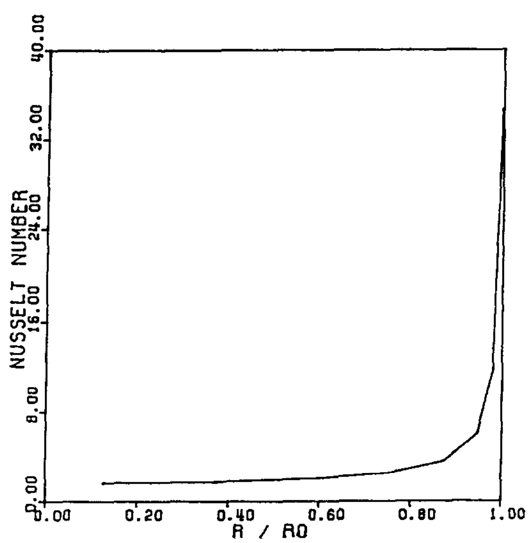

FIG. 3. Nusselt number plot for $Gr = 10^4$, $Da = 10^5$ and $Vo = 0$.

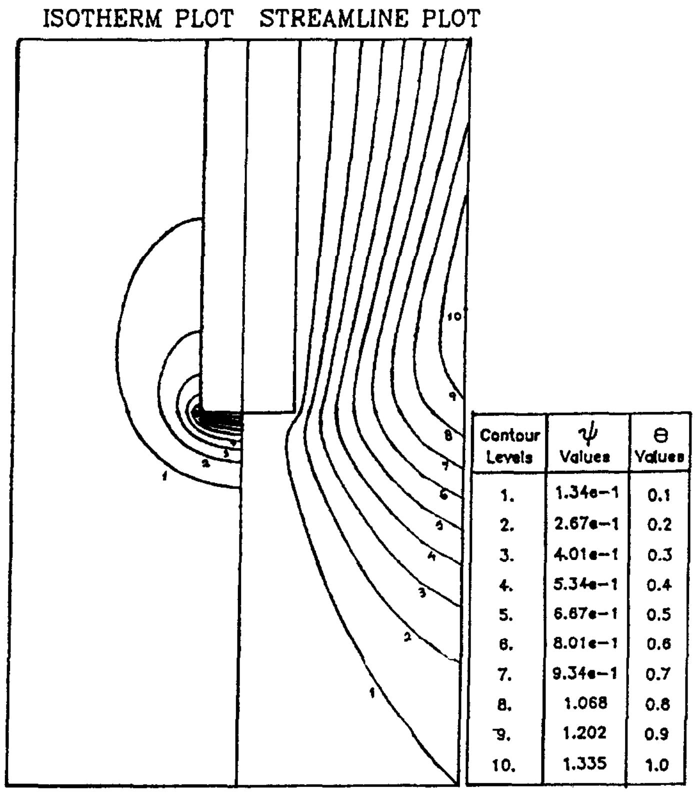

Contour Levels	ψ Values	θ Values
1.	1.34e−1	0.1
2.	2.67e−1	0.2
3.	4.01e−1	0.3
4.	5.34e−1	0.4
5.	6.67e−1	0.5
6.	8.01e−1	0.6
7.	9.34e−1	0.7
8.	1.068	0.8
9.	1.202	0.9
10.	1.335	1.0

FIG. 4. Streamline and isotherm plot for $Gr = 10^4$, $Da = 10^4$ and $Vo = 0$.

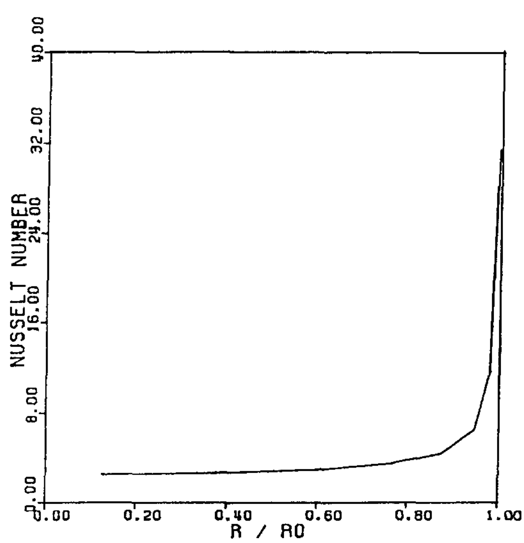

FIG. 5. Nusselt number plot for $Gr = 10^4$, $Da = 10^4$ and $Vo = 0$.

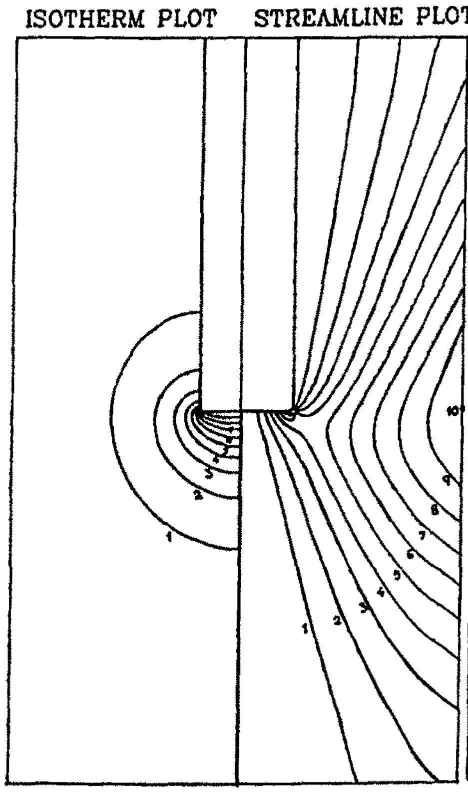

Contour Levels	ψ Values	θ Values
1.	1.43e-3	0.1
2.	2.87e-3	0.2
3.	4.30e-3	0.3
4.	5.74e-3	0.4
5.	7.17e-3	0.5
6.	8.61e-3	0.6
7.	1.00e-3	0.7
8.	1.14e-2	0.8
9.	1.29e-2	0.9
10.	1.43e-2	1.0

FIG. 6. Streamline and isotherm for $Gr = 10^4$, $Da = 10^6$ and $Vo = 5000$.

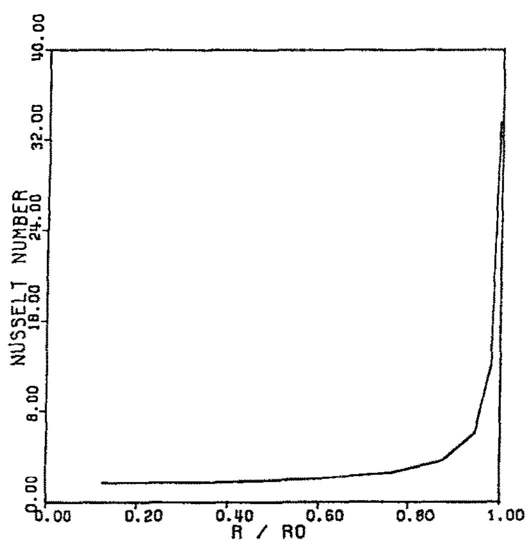

FIG. 7. Nusselt number plot for $Gr = 10^4$, $Da = 10^6$ and $Vo = 5000$.

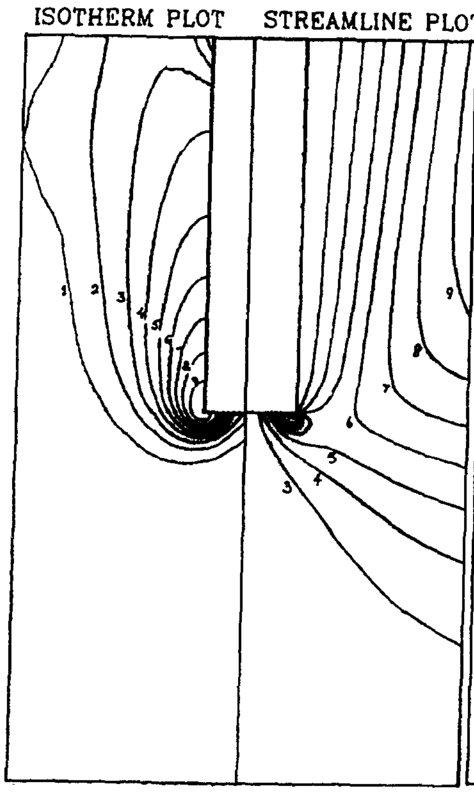

Contour Levels	ψ Values	Θ Values
1.	0.561	0.1
2.	1.124	0.2
3.	1.685	0.3
4.	2.247	0.4
5.	2.809	0.5
6.	3.371	0.6
7.	3.930	0.7
8.	4.490	0.8
9.	5.056	0.9
10.	5.618	1.0

FIG. 8. Streamline and isotherm plot for $Gr = 10^4$, $Da = 10^4$ and $Vo = 5000$.

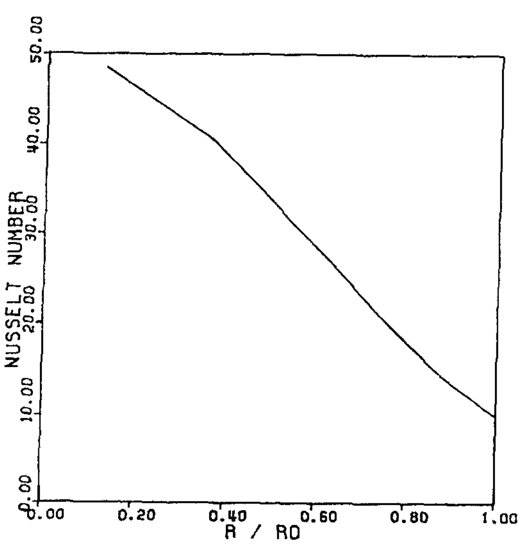

FIG. 9. Nusselt number plot for $Gr \approx 10^4$, $Da = 10^4$ and $Vo = 5000$.

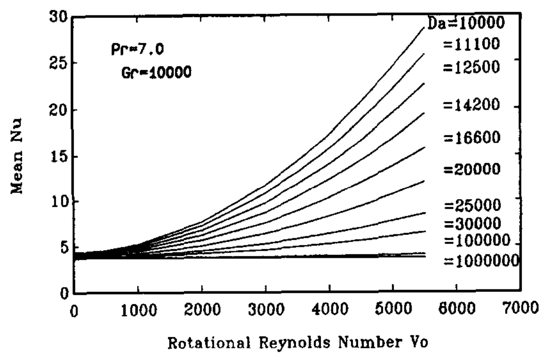

FIG. 10. Correlation for mean Nusselt number.

takes over at high rotational speeds for a given Darcy number.

Acknowledgement—The ANSYS package is the registered trademark of Swanson Analysis System, Inc.

REFERENCES

1. W. J. Minkowycz and P. Cheng, Free convection about a vertical cylinder embedded in a porous medium, *J. Heat Transfer* **19**, 805 (1979).
2. H. H. Bau, Low Rayleigh number thermal convection in a saturated porous medium bounded by two horizontal eccentric cylinders, *J. Heat Transfer* **106**, 167 (1984).
3. P. J. Burns and C. L. Tien, Natural convection in porous media bounded by concentric spheres and horizontal cylinders, *Int. J. Heat Mass Transfer* **22**, 929 (1979).
4. T. H. Kuehn and R. J. Goldstein, An experimental study of natural convection heat transfer in concentric and eccentric horizontal cylindrical annuli, *J. Heat Transfer* **100**, 635 (1978).
5. A. Nakayama and H. Koyama, A general similarity transformation for combined free and forced convection flows within a fluid saturated porous medium, *J. Heat Transfer* **109**, 1042 (1987).
6. K. Vafai and C. L. Tien, Boundary and inertia effects on flows and heat transfer in porous media, *Int. J. Heat Mass Transfer* **24**, 195 (1981).
7. V. Prasad and G. Lauriat, Natural convection in a vertical porous cavity: a numerical study for Brinkmann extended Darcy formulation, *J. Heat Transfer* **109**, 688 (1987).
8. M. R. Ravi, M.E. Thesis, Indian Institute of Science, Bangalore (1988).
9. S. V. Patankar, *Numerical Heat Transfer and Fluid Flow*. Hemisphere, New York (1980).
10. M. R. Ravi and A. G. Marathe, *Int. Heat Transfer Conf. IHTC-9*, Jerusalem, Israel, Vol. 2, p. 129 (1990).
11. S. V. Patankar and D. B. Spalding, A calculation procedure for heat, mass and momentum transfer in 3-d parabolic flows, *Int. J. Heat Mass Transfer* **15**, 1777 (1972).
12. M. Carter, *Geotechnical Engineering Handbook*. Pentech Press, London (1980).

TRANSFERT CONVECTIF A LA BASE D'UN CYLINDRE PIVOTANT AUTOUR D'UN AXE VERTICAL DANS UN MILIEU POREUX SATURE

Résumé—On étudie numériquement le transfert thermique à la base d'un cylindre pivotant autour d'un axe vertical dans un milieu saturé poreux. Le problème est axisymétrique. Les équations sans dimension sont résolues avec l'algorithme SIMPLER sur une grille étagée. L'influence des nombres de Reynolds rotationnel et de Darcy sur le transfert thermique est étudiée pour un nombre de Grashof de 10^4 et un nombre de Prandtl de 7. On trouve que pour des nombres de Darcy très élevés, le transfert est principalement de conduction pour un large domaine de nombre de Rayleigh rotationnel. Le transfert convectif prend place aux faibles nombres de Darcy et pour les nombres de Reynolds rotationnel les plus élevés. Néanmoins, il y a un accroissement rapide du nombre de Nusselt global au dessous d'un certain nombre de Darcy avec l'accroissement du nombre de Reynolds rotationnel. L'effet du nombre de Darcy et du nombre de Reynolds rotationnel sur le transfert thermique et l'écoulement dans le milieu poreux est décrit par des cartes d'isothermes et de lignes de courant. On trace la variation du nombre de Nusselt global relativement au nombre de Darcy pour plusieurs nombres de Reynolds rotationnels. On donne la variation du nombre de Nusselt local, pour la coordonnée radiale de l'extrémité chauffée du cylindre vertical, pour plusieurs nombres de Darcy et de Reynolds rotationnel.

KONVEKTIVER WÄRMEÜBERGANG AM BODEN EINES UM SEINE VERTIKALE ACHSE IN EINEM GESÄTTIGTEN PORÖSEN MEDIUM ROTIERENDEN ZYLINDERS

Zusammenfassung—Es wird der Wärmeübergang an der Unterseite eines Zylinders numerisch untersucht. Der Zylinder rotiert um seine vertikale Achse und befindet sich in einem unendlich ausgedehnten, gesättigten porösen Medium. Das Problem ist achsensymmetrisch. Die Erhaltungsgleichungen werden dimensionlos gemacht und mit Hilfe des SIMPLER-Algorithmus mit einem gestuften Gitternetz gelöst. Es wird der Einfluß der Rotations-Reynolds-Zahl und der Darcy-Zahl auf den Wärmeübergang für eine Grashof-Zahl von 10^4 und eine Prandtl-Zahl von 7,0 untersucht. Für sehr große Darcy-Zahlen zeigt sich in einem weiten Bereich der Rotations-Reynolds-Zahl, daß der Wärmetransport hauptsächlich auf Wärmeleitung beruht. Konvektiver Wärmetransport findet bei kleiner Darcy-Zahl und größeren Rotations-Reynolds-Zahlen statt. Darüberhinaus nimmt die Gesamt-Nusselt-Zahl unterhalb einer gewissen Darcy-Zahl mit zunehmender Rotations-Reynolds-Zahl rasch zu. Der Einfluß der Darcy- und der Rotations-Reynolds-Zahl auf den Wärmeübergang und die Strömung in einem porösen Medium wird in Form von Stromlinien und Isothermen gezeigt. Insbesondere wird die Veränderung der Gesamt-Nusselt-Zahl in Abhängigkeit von der Darcy-Zahl für verschiedene Rotations-Reynolds-Zahlen dargestellt. Abschließend wird der Verlauf der örtlichen Nusselt-Zahl an der beheizten Oberseite des vertikalen Zylinders in radialer Richtung für verschiedene Darcy- und Rotations-Reynolds Zahlen gezeigt.

КОНВЕКТИВНЫЙ ТЕПЛОПЕРЕНОС ОТ ОСНОВАНИЯ ЦИЛИНДРА, ВРАЩАЮЩЕГОСЯ ВОКРУГ ВЕРТИКАЛЬНОЙ ОСИ В НАСЫЩЕННОЙ ПОРИСТОЙ СРЕДЕ

Аннотация—Численно исследуются характеристики теплопереноса от основания цилиндра, вращающегося вокруг вертэкальной оси в бесконечной насыщенной пористой среде. Задача является осесимметричной. Безразмерные определяющие уравнения решаются с использованием алгоритма SIMPLER. Исследуется влияние вращательных чисел Рейнольдса и чисел Дарси на теплоперенос при числе Грасгофа, равном 10^4 и числе Прандтля, равном 7,0. Найдено, что при очень больших числах Дарси в широком диапазоне вращательных чисел Рейнольдса теплоперенос происходит преимущественно за счет теплопроводности. Конвективный перенос тепла осуществляется при более низких числах Дарси и больших вращательных числах Рейнольдса. Кроме того, при числах Дарси меньше определенного значения наблюдается резкое увеличение числа Нуссельта с ростом вращательного числа Рейнольдса. Влияние числа Дарси и вращательного числа Рейнольдса на теплоперенос и течение жидкости в пористой среде иллюстрируется графически в виде линий тока и изотерм. Приводятся графики изменений числа Нуссельта в зависимости от числа Дарси при различных вращательных числах Рейнольдса. Даются также графики изменения локального числа Нуссельта как функции радиальной координаты у нагретого основания вертикального цилиндра при различных числах Дарси и вращательных числах Рейнольдса.